IEEE Access
Multidisciplinary ⋮ Rapid Review ⋮ Open Access Journal

Received 25 September 2025, accepted 18 October 2025, date of publication 22 October 2025, date of current version 28 October 2025.

Digital Object Identifier 10.1109/ACCESS.2025.3624368

RESEARCH ARTICLE

A New Parameterization of a MARV for Adaptive Control in Backward Movements

DIEGO NUNES BERTOLANI[1], RICARDO CARELLI[2], (Senior Member, IEEE), AND MÁRIO SARCINELLI-FILHO[3]

[1]Instituto Federal de Educação, Ciência e Tecnologia do Espírito Santo, Campus Guarapari, Guarapari, Espírito Santo 29216-795, Brazil
[2]Instituto de Automática, Universidad Nacional de San Juan, San Juan J5400, Argentina
[3]Departamento de Engenharia Elétrica, Universidade Federal do Espírito Santo, Vitoria, Espírito Santo 29075-910, Brazil

Corresponding author: Mário Sarcinelli-Filho (mario.sarcinelli@ufes.br)

This work was supported in part by CNPq - Conselho Nacional de Desenvolvimento Científico e Tecnológico, Brazil (grant number 305726/2021-8), and in part by FAPES-ES - Fundação de Amparo à Pesquisa e Inovação do Espírito Santo, Brazil (grant number TO 987/20222).

ABSTRACT This study introduces a simplified parametric model of the backward movements of a Multi-articulated Robotic Vehicle (MARV). The model underwent simulation testing and experimental validation, considering a MARV setup comprising a tractor and a trailer with varying loads. This scenario mirrors situations such as truck-trailer maneuvers in reverse or applications involving a tractor moving a passive trailer in settings like ports, airports, or warehouses. The primary concern is enabling these articulated vehicles to navigate without collisions between their components (referred to as *jackknife*), which could halt their movement. The experiments utilized a pre-existing adaptive dynamic controller to assess whether incorporating new parameters about the trailer's influence on the tractor element within the differential robot model could enhance MARV navigation. This approach aims to develop a more accurate model for MARV, taking into account the effects of loaded and unloaded trailers. The findings indicate that accounting for these effects reduces navigation errors, albeit at the expense of marginally increased model complexity.

INDEX TERMS Multi-articulated robotic vehicle, parametric model, nonlinear control, robot model, mobile robotics.

I. INTRODUCTION

This study delves into controlling multi-articulated robotic vehicles, known as MARVs. Equipped with autonomous navigation systems, these vehicles execute maneuvers relevant to various applications. Navigating these robots, especially during backward movements, poses a significant challenge due to the potential occurrence of *jackknife* situations, in which the vehicle's motion is halted — a scenario to be avoided.

The primary aim is to develop tools aiding human operators in navigating MARVs during complex maneuvers, particularly in reverse. Advancements in this domain could lead to cost reductions and enhanced efficiency in industrial and agricultural settings [1], particularly in logistics and cargo transportation. This is crucial because utilizing a single MARV (a truck with trailers) incurs lower operational costs than employing multiple individual trucks. However, navigating MARVs presents a formidable challenge due to their complex, nonlinear nature, as they are under-actuated systems with intricate kinematics and dynamics [2].

Several control methodologies have been implemented to guide MARVs autonomously, spreading from simpler ones, like time-varying linear quadratic regulator [3], feedback linearization [4], to more complex ones, relying on neural networks [5], [6], and fuzzy logic [7], [8]. There are also approaches exploring modularity [9], employing adaptive control [10], [11], sliding mode control [12], [13], and predictive control [14], [15], whose adoption is much likely determined by the highly nonlinear behavior of the MARV, which poses challenges in precise modeling, inherent to the use of feedback linearization, for instance.

This study focuses on refining the modeling of MARVs by proposing a new parameterized model for tractor dynamics,

The associate editor coordinating the review of this manuscript and approving it for publication was Zheng Chen.

© 2025 The Authors. This work is licensed under a Creative Commons Attribution 4.0 License.
For more information, see https://creativecommons.org/licenses/by/4.0/

which takes into account the impact of attached trailers. Traditionally, MARV modeling, as seen in [4] and [11], for instance, has employed the classical dynamic model of the differential robot, used as the tractor, without accounting for the influence of the trailers. Therefore, the main contribution of the paper is the proposition of a model that considers the influence of the passive trailers on the dynamics of the tractor robot, albeit in a simplified manner. In other words, the focus of the study is to answer the question ''Does the model previously published (see [11]) suitably represent the dynamics of the tractor robot, mainly when the MARV transports heavier payloads?''. The proposed hypothesis is that such a model is insufficient to ensure the controller's good performance, as demonstrated by the experiments conducted here. Then, our proposal is to introduce two new parameters to account for the influence of the trailer on the tractor, represented by θ_7 and θ_8. The results of the experiments, which considered an adaptive controller based on a model with just 6 parameters and the new model with 8 parameters, show a meaningful difference in system performance for increased payloads. However, accurately capturing this influence is a challenge. As a first step towards contributing to a more comprehensive MARV model, this research considers a MARV configuration consisting of a differential robot and a single trailer. It introduces two additional parameters into the dynamic model of the tractor to represent the trailer's influence and proposes a model based on eight parameters. In experimental trials involving eight different loads, the effectiveness of the adaptive dynamic control system developed in [11] in adapting to these new parameters is examined. The results are compared with those from the same MARV setup, excluding the two new parameters associated with the influence of the trailer, as described in [11]. Achieving a control system that significantly reduces control errors is crucial to the task's performance, particularly when operating in constrained spaces. Thus, the investigation assesses whether increased model complexity enhances system performance, particularly in terms of position error, justifying its adoption. The result is a significant reduction in position error when using the new model proposed in this paper, which is its first contribution. In addition, the paper generalizes the dynamic model of the tractor robot to account for the influence of multiple trailers, a meaningful additional contribution.

To discuss the topics involved, the remaining text is organized into four sections. Section II delves into the structure of the robot-trailer(s), detailing their geometry and the interplay of angular and linear velocities within the articulated chain. It also revisits the kinematic model of each MARV element, all of which are nonholonomic vehicles. Furthermore, this section introduces a novel dynamic model for the tractor element of the MARV, now incorporating the influence of the trailer(s). Moving forward, Section III outlines how to implement the dynamic adaptive control structure, now considering the new dynamic model of the tractor element. Subsequently, Section IV presents the outcomes obtained by comparing the performance of the complete control system, utilizing the new dynamic tractor model, with that based on the classical dynamic model, and Section V generalizes the proposed system for n trailers. Finally, Section VI summarizes the key findings and conclusions drawn from the study.

In summary, the focus of the paper is on developing a more precise dynamic model for the tractor element of the MARV, which includes two specific parameters to account for the additional effort required to move one trailer. The more suitable comparison, therefore, is with the model adopted in [11], which considers just the dynamics of the tractor element, disregarding the influence of the trailer. The paper's primary objective is to validate this hypothesis, which is effectively achieved. In a second moment, the paper extends this new model to account for the presence of two trailers, and generalizes the model formulation to consider n trailers.

In terms of model validation, the paper considers its use in designing an adaptive controller, which is essentially the same as that adopted in [11]. This approach allows for a fair comparison of the two models, which are essential components of the designed controllers. Moreover, the reason for adopting an adaptive controller is that the applications of MARVs in load transportation often involve different payloads in each task. For instance, in the case of luggage transportation from the terminal to the aircraft in airports, where MARVs are commonly adopted, each flight requires a different payload. As is well known, adaptive control allows for correcting the model parameters mapped into the control law; however, it has limitations because it does not permit changing the model structure, only changing parameter values, which limits its capability to achieve better performance. In several cases, such as when the payload undergoes significant changes, it is necessary to obtain an enhanced model to achieve better performance in task accomplishment, as demonstrated by the experiments reported here.

II. MARV DESCRIPTION AND MODELING

A. MARV STRUCTURE

This study employs the widely recognized differential-drive mobile robot *Pioneer 3-DX* as the tractor component of the MARV, which is configured to push one or more trailers (passive elements incapable of self-propulsion), as depicted in Figure 1. Therefore, the control signals designed to navigate the MARV should be delivered to such a robot.

In terms of geometry, as detailed in [11] (from where Figure 1 is sourced), L_{0_0}, L_{1_0}, $L_{2_0}, \cdots, L_{n-1_0}$ represents the distances between the midpoint of the axle of one element and the hitch point of the subsequent one. Meanwhile, L_i, $i = 1, 2, \cdots, n-1, n$, denotes the distance between the midpoint of the axle of the i-th trailer and its frontal hitching point. Additionally, b signifies the distance from the midpoint of the

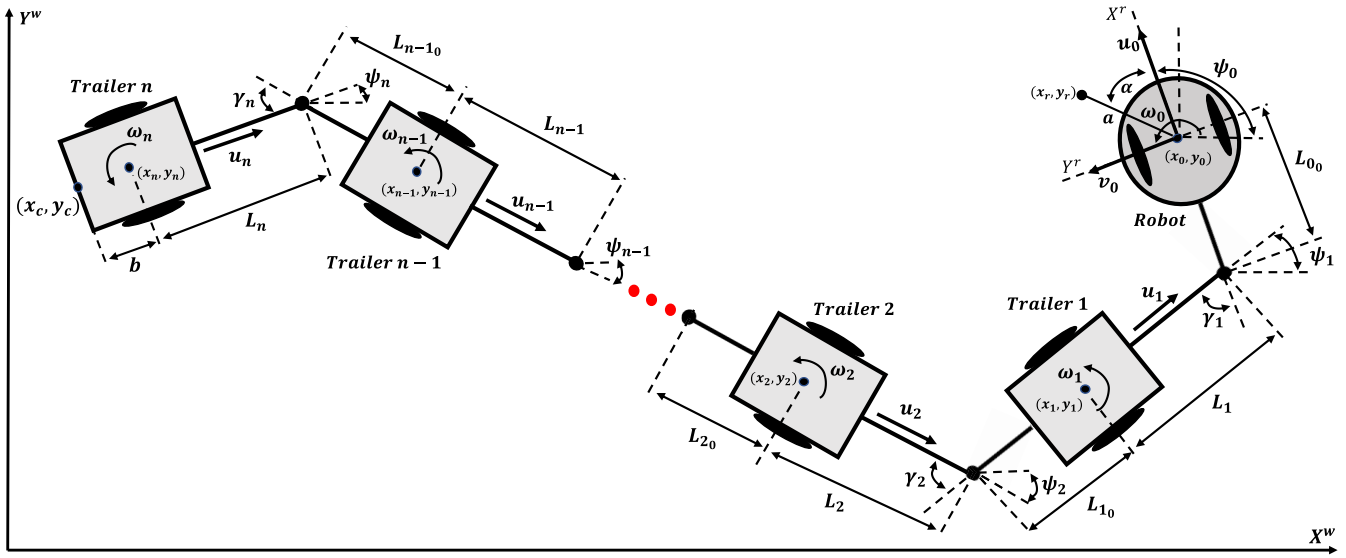


FIGURE 1. A sketch of a MARV having n trailers, showing the geometric/angular parameters and velocities involved (see [11]).

last axle and the PoI (point of interest for control), located at $(x_c,\ y_c)$ in the middle of the rear section of the final trailer, which requires control over its position. The coordinates $(x_i,\ y_i)$, $i = 0, 1, 2, \cdots, n-1, n$, represent the midpoint of the axle of the i-th element, while (x_r, y_r) denotes the coordinates of a generic PoI rigidly attached to the tractor element, in the inertial frame.

Furthermore, u_i, $i = 0, 1, 2, \cdots, n-1, n$, denote the linear velocities along the longitudinal axis of the i-th MARV element, and ω_i, $i = 0, 1, 2, \cdots, n-1, n$, represent the angular velocities for these elements, with positive values indicating counterclockwise rotation. Similarly, ψ_i, $i = 0, 1, 2, \cdots, n-1, n$, denote the orientation of each MARV element relative to the axis X^W of the inertial frame, also measured positively in a counterclockwise direction. Lastly, γ_i, $i = 1, 2, \cdots, n$, refer to the angles between consecutive MARV elements, with positive values indicating counterclockwise rotation.

The coordinates (x_c, y_c) of the PoI are derived from the midpoint coordinates of the axle of the final element within the assembly. This relationship is expressed as

$$\begin{bmatrix} x_c \\ y_c \end{bmatrix} = \begin{bmatrix} x_n \\ y_n \end{bmatrix} - b \begin{bmatrix} \cos\psi_n \\ \sin\psi_n \end{bmatrix}. \tag{1}$$

Additionally, referencing Figure 1, one can establish the relationship

$$\begin{bmatrix} x_i \\ y_i \end{bmatrix} = \begin{bmatrix} x_{i-1} \\ y_{i-1} \end{bmatrix} - L_{i-1_0} \begin{bmatrix} \cos\psi_{i-1} \\ \sin\psi_{i-1} \end{bmatrix} - L_i \begin{bmatrix} \cos\psi_i \\ \sin\psi_i \end{bmatrix}, \tag{2}$$

for $i = 1, \cdots, n$, thereby establishing the connection between the midpoint coordinates of the axle of the i-th trailer and that of the $(i-1)$-th trailer. Consequently, this enables the determination of the midpoint coordinates of the axles for each trailer, starting from the tractor element (referred to as the robot) and moving towards the trailers. Furthermore, by examining Figure 1, the angular relationships can be expressed as

$$\gamma_i = \psi_{i-1} - \psi_i, \quad i = 1, \cdots, n. \tag{3}$$

B. VELOCITY RELATIONSHIPS

The kinematic model adopted here for the differential drive robot is that of [16]. It considers a PoI placed anywhere, however rigidly coupled to the robot, apart from a m of the midpoint of its virtual axle and rotated α degrees/rads concerning the axis X^r of the robot frame (see the point $(x_r,\ y_r)$ in Figure 1).

To regulate the movement of the PoI, situated within the final trailer, it is imperative to govern the motion of each preceding trailer. This is achieved by adopting the same kinematic model used for the robot, since the trailers are nonholonomic platforms, meaning they cannot move in line with their axles. The sole contrast lies in the absence of traction capability within the trailers. Thus, conceiving the system as a sequence of n robots sharing an identical kinematic model is essential. Consequently, in devising the controller, it is crucial to account for the PoI within the last trailer, positioned at a distance b from the center of its axle, and to produce control signals that induce the desired motion of such point, denoted as (x_c, y_c). Subsequently, these control signals must be transmitted to the leading tractor unit, specifying its movement to ensure the desired motion of the point (x_c, y_c).

The relationship between the velocities of the elements of the articulated chain, from the last trailer to the tractor element, is a generalization of the one between the velocities of two consecutive MARV elements. For the i-th and the $(i-1)$-th trailers such a relationship is given by [17]

and [18],

$$\underbrace{\begin{bmatrix} u_{i-1} \\ \omega_{i-1} \end{bmatrix}}_{\mathbf{u}_{i-1}} = \underbrace{\begin{bmatrix} \cos\gamma_i & L_i \sin\gamma_i \\ \frac{\sin\gamma_i}{L_{i-1_0}} & -\frac{L_i \cos\gamma_i}{L_{i-1_0}} \end{bmatrix}}_{{}^{(i-1)}\mathbf{T}_{(i)}} \underbrace{\begin{bmatrix} u_i \\ \omega_i \end{bmatrix}}_{\mathbf{u}_i} = {}^{(i-1)}\mathbf{T}_{(i)}\mathbf{u}_i, \quad (4)$$

for $i = n, n-1, \cdots, 2, 1$ ($n \geq 1$), where ${}^{(i-1)}\mathbf{T}_{(i)}$ is a nonsingular matrix, since its determinant is $-L_i/L_{i-1_0} \neq 0$. The extension to the entire composition results in [11]

$$\mathbf{u}_0 = {}^{(0)}\mathbf{T}_{(1)}\, {}^{(1)}\mathbf{T}_{(2)} \cdots {}^{(n-1)}\mathbf{T}_{(n)}\mathbf{u}_n = {}^{(0)}\mathbf{T}_{(n)}\mathbf{u}_n, \quad (5)$$

which gives the velocities the tractor element should develop to move the PoI $(x_c,\ y_c)$ accordingly. An important remark is that ${}^{(0)}\mathbf{T}_{(n)}$ is a nonsingular matrix so that its inverse exists. Therefore, $\mathbf{u}_n = [{}^{(0)}\mathbf{T}_{(n)}]^{-1}\mathbf{u}_0 = {}^{(n)}\mathbf{T}_{(0)}\mathbf{u}_0$ is also a valid relationship.

C. KINEMATIC MODELS

According to [16], the characterization of the movement of the point $(x_r,\ y_r)$ shown in Figure 1 follows

$$\begin{bmatrix} \dot{x}_r \\ \dot{y}_r \\ \dot{\psi}_0 \end{bmatrix} = \begin{bmatrix} \cos\psi_0 & -\sin\psi_0 & -a\sin(\alpha+\psi_0) \\ \sin\psi_0 & \cos\psi_0 & a\cos(\alpha+\psi_0) \\ 0 & 0 & 1 \end{bmatrix} \begin{bmatrix} u_0 \\ v_0 \\ \omega_0 \end{bmatrix}, \quad (6)$$

where u_0 is the longitudinal linear velocity of the robot, v_0 is its linear velocity in line with its virtual axle, a fictitious velocity, because the robot is a nonholonomic vehicle, and ω_0 is its angular velocity. However, the objective here is to design a controller for the PoI in the last trailer. However, as nonholonomic vehicles, the trailers have kinematic models similar to the one in (6). Therefore, the kinematic model for the last trailer, for which $a = b$ and $\alpha = 180°$, is

$$\begin{bmatrix} \dot{x}_n \\ \dot{y}_n \\ \dot{\psi}_n \end{bmatrix} = \begin{bmatrix} \cos\psi_n & -\sin\psi_n & -b\sin(180° + \psi_n) \\ \sin\psi_n & \cos\psi_n & b\cos(180° + \psi_n) \\ 0 & 0 & 1 \end{bmatrix} \begin{bmatrix} u_n \\ v_n \\ \omega_n \end{bmatrix}, \quad (7)$$

which will be used to design the controller that will generate the velocity commands u_n and ω_n for the last trailer, besides guaranteeing the nonholonomic condition $v_n = 0$.

D. KINEMATIC CONTROLLER FOR THE LAST TRAILER

The kinematic controller designed for the last trailer is based on the feedback linearization strategy [19], considering just the inverse kinematics of this MARV element, in which the PoI is. Such a design assumes perfect velocity tracking, meaning the vehicle's velocity instantaneously assumes the commanded value. The result is that control errors arise, referring to the PoI position, mainly when the trailers are loaded. The kinematic control law adopted is the same one adopted in [4] and [11], for which the commanded velocities are, imposing that $v^k_{n_{ref}} = 0$, thus fulfilling the nonholonomic restriction,

$$u^k_{n_{ref}} = V_x \cos\psi_n + V_y \sin\psi_n + V_\psi b \sin\alpha, \text{ and} \quad (8)$$

$$\omega^k_{n_{ref}} = V_\psi, \quad (9)$$

where $V_x = \dot{x}_{c_d} + k_{px}(x_{c_d} - x_c)$, $V_y = \dot{y}_{c_d} + k_{py}(y_{c_d} - y_c)$ and $V_\psi = \frac{-V_x \sin\psi + V_y \cos\psi}{a\cos\alpha}$, with (x_{c_d}, y_{c_d}) being the desired position of the PoI and (x_c, y_c) being its current position (see [19]). Such control signals are then propagated to the tractor element using (5), thus getting the velocity references $u^k_{0_{ref}}$ and $\omega^k_{0_{ref}}$ for the tractor element.

E. DYNAMIC MODEL OF THE DIFFERENTIAL ROBOT

The dynamic model employed for the robot in question is derived from prior research [4], [20]. It can be expressed as

$$\begin{bmatrix} \dot{u}_0 \\ \dot{\omega}_0 \end{bmatrix} = \begin{bmatrix} \frac{\theta_3}{\theta_1}\omega_0^2 - \frac{\theta_4}{\theta_1}u_0 \\ -\frac{\theta_5}{\theta_2}u_0\omega_0 - \frac{\theta_6}{\theta_2}\omega_0 \end{bmatrix} + \begin{bmatrix} \frac{1}{\theta_1} & 0 \\ 0 & \frac{1}{\theta_2} \end{bmatrix} \begin{bmatrix} u_{0_{ref}} \\ \omega_{0_{ref}} \end{bmatrix}, \quad (10)$$

where $u_{0_{ref}}$ and $\omega_{0_{ref}}$ denote the control signals, and θ_i, $i = 1, \cdots, 6$, represent parameters of the dynamic model of the robot, such as mass, moment of inertia, Coulomb friction, motor constants, and servo controller gains. However, obtaining precise values for these parameters is challenging, as they involve numerous physical characteristics of the robot that are often undisclosed by the manufacturer. Moreover, measuring them is intricate due to the complex interplay of dynamic effects they represent. To address this, an identification procedure was undertaken solely on the tractor element, yielding the estimates $\hat{\theta}_1 = 0.23882$ s, $\hat{\theta}_2 = 0.23938$ s, $\hat{\theta}_3 = 0.0038418$ sm/rad^2, $\hat{\theta}_4 = 0.9435$, $\hat{\theta}_5 = -0.007849$ s/m, and $\hat{\theta}_6 = 0.92249$ for the dynamic parameters.

The differential drive robot's complete model combines kinematic and dynamic aspects. Despite their interdependence, these modules can be treated separately, enabling the design of a controller using an inner-outer loop structure. However, this control structure varies slightly for the Multi-Articulated Robotic Vehicle (MARV). The kinematic controller, designed using the feedback linearization technique, considers the kinematics of the last trailer, producing velocity commands that are propagated through the chain to get u_0 and ω_0 for the tractor element. Meanwhile, the inner loop involves a dynamic controller tailored for the tractor element, as outlined in [21]. This setup ensures that the tractor element receives velocity commands derived from the overall MARV kinematics, allowing coordinated motion according to the specified task. At the same time, its dynamics is partially compensated by the dedicated inner control loop [4], [11].

F. THE NEW DYNAMIC MODEL ACCOUNTING FOR THE TRAILERS

So far, the dynamic compensation considers that the dynamics of the tractor element is not influenced by the trailers attached to it [11]. Although simplifying the design of the controller, this strategy may generate significant errors when loading the trailers, for instance. To account for this, the trailers' influence on the composition's movement is considered here, although in a simplified way. Firstly, the effect of one trailer on the tractor, which is concentrated as longitudinal and transversal forces in the junction between

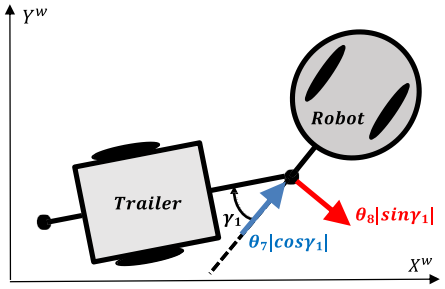


FIGURE 2. The proposed strategy to include the trailer's influence in the dynamics of the tractor element, for a MARV with one trailer.

the tractor element and the first trailer, as shown in Figure 2, is considered. After, a generalization for n trailers is presented in Section V.

Manipulating (10) one can write

$$\begin{bmatrix} u_{0_{ref}} \\ \omega_{0_{ref}} \end{bmatrix} = \begin{bmatrix} \theta_1 & 0 \\ 0 & \theta_2 \end{bmatrix} \begin{bmatrix} \dot{u}_0 \\ \dot{\omega}_0 \end{bmatrix} + \mathbf{B}\theta, \tag{11}$$

with $\mathbf{B} = \begin{bmatrix} 0 & 0 & -\omega_0^2 & u_0 & 0 & 0 \\ 0 & 0 & 0 & 0 & \omega_0 u_0 & \omega_0 \end{bmatrix}$, and $\theta = \begin{bmatrix} \theta_1 & \theta_2 & \theta_3 & \theta_4 & \theta_5 & \theta_6 \end{bmatrix}^T$. In matrix notation one has

$$\mathbf{v}_{ref} = \mathbf{D}\dot{\mathbf{v}} + \eta \tag{12}$$

where $\mathbf{v}_{ref} = \begin{bmatrix} u_{0_{ref}} & \omega_{0_{ref}} \end{bmatrix}^T$, $\mathbf{D} = diag(\theta_1, \theta_2)$, $\dot{\mathbf{v}} = \begin{bmatrix} \dot{u}_0 & \dot{\omega}_0 \end{bmatrix}^T$, and $\eta = \mathbf{B}\theta$.

The effect caused by the trailer on the tractor robot is considered as two forces, as Figure 2 illustrates. These forces come from the decomposition of the reaction force that the trailer applies to the tractor. Two new parameters are considered to account for the interaction force between the tractor and the trailer. Thus, $\sigma_1 = \theta_7|cos\gamma_1|$ accounts for the effect of the trailers on the linear acceleration of the robot, whereas $\sigma_2 = \theta_8|sin\gamma_1|$ accounts for their effect on the angular acceleration of the tractor element. These terms aim to model the inertial effects of the trailer on the tractor, which is a dominant dynamic effect that must be taken into account. Notice that the angle γ_1 is supposed to be always lower than 90° to avoid jackknife, so that even when the first trailer is at the right of the trailer, a situation in which the red vector in Figure 2 would point to the left, one would get the angle $-\gamma_1$, instead of γ_1, to calculate σ_1, and $\gamma_1 + 90°$, instead of γ_1, to calculate σ_2. Anyway, the values of the cos and sin would be the same, always positive, thus corresponding to $|\cos\gamma_1|$ and $|\sin\gamma_1|$. With such considerations, one can write the new dynamic model as

$$\begin{bmatrix} u_{0_{ref}} \\ \omega_{0_{ref}} \end{bmatrix} = \left[\begin{pmatrix} \theta_1 & 0 \\ 0 & \theta_2 \end{pmatrix} + \begin{pmatrix} \sigma_1 & 0 \\ 0 & \sigma_2 \end{pmatrix} \right] \begin{bmatrix} \dot{u}_0 \\ \dot{\omega}_0 \end{bmatrix} + \mathbf{B}^\dagger\theta, \tag{13}$$

or, in matrix notation,

$$\mathbf{v}_{ref} = \mathbf{D}^\dagger\dot{\mathbf{v}} + \eta^\dagger, \tag{14}$$

which is similar to (12), now with $\mathbf{D}^\dagger = diag(\theta_1 + \theta_7|cos\gamma_1|, \theta_2 + \theta_8|sin\gamma_1|)$, $\eta^\dagger = \mathbf{B}^\dagger\theta$, $\mathbf{B}^\dagger = \begin{bmatrix} 0 & 0 & -\omega_0^2 & u_0 & 0 & 0 & 0 & 0 \\ 0 & 0 & 0 & 0 & \omega_0 u_0 & \omega_0 & 0 & 0 \end{bmatrix}$ and the new vector of parameters $\theta = \begin{bmatrix} \theta_1 & \theta_2 & \theta_3 & \theta_4 & \theta_5 & \theta_6 & \theta_7 & \theta_8 \end{bmatrix}^T$. Moreover, from such an equation one can perceive that σ_1 and σ_2, and thus θ_7 and θ_8, are dimensionless values, with θ_7 and θ_8 being constants to be identified.

Therefore, in this section, the kinematic model for an MARV with n trailers and the dynamic model for the case of one trailer have been obtained, and will be used in the following section to design an adaptive controller for the single robot-trailer configuration. A generalization of the design for an MARV with n trailers is presented in Section V.

III. ADAPTIVE DYNAMIC COMPENSATION

The adaptive dynamic controller proposed here resembles the one introduced in [11] (refer to the provided block diagram), incorporating a kinematic controller and a dynamic compensator. This compensator leverages the decoupling of kinematics and dynamics [21], [22], alongside a parameter updating law. The kinematic controller generates velocity references for the last trailer of the assembly (a passive element), which are then transmitted to the tractor element (robot). Subsequently, dynamic compensation is executed on the tractor robot, now considering the updated parameter set $\theta_1, \cdots, \theta_8$. Notably, this approach accounts for the influence of the trailers on the tractor robot. While the design of the kinematic controller mirrors that of [11], the focus here is solely on the design of the dynamic compensator.

Initiating such a design involves utilizing the velocity references $u_{0_{ref}}^k$ and $\omega_{0_{ref}}^k$ provided by the kinematic controller intended for the last trailer, yet transmitted to the tractor robot. However, the robot does not immediately adopt these velocities, leading to a velocity-tracking error caused by dynamic factors such as friction, mass, inertia, internal forces, torques, and disturbances. This error varies based on the robot's dynamics. Thus, developing a dynamic compensator becomes crucial to alter these dynamics, aiming to reduce the velocity tracking error more swiftly and enhance the maneuverability of the entire articulated chain. Since it is the sole active element in the assembly, dynamic compensation is confined to the tractor robot. Nevertheless, all passive elements are expected to be influenced by the compensation applied to the robot dynamics, which results from the enhanced performance of the tractor element.

Therefore, what is proposed here is an extension of the dynamic controller of [21], now considering the new model of (14). The control law adopted is

$$\begin{bmatrix} u_{0_{ref}} \\ \omega_{0_{ref}} \end{bmatrix} = \begin{bmatrix} \hat{\theta}_1 + \hat{\theta}_7|cos\gamma_1| & 0 \\ 0 & \hat{\theta}_2 + \hat{\theta}_8|sin\gamma_1| \end{bmatrix} \begin{bmatrix} \delta_1 \\ \delta_2 \end{bmatrix} + \mathbf{B}^\dagger\hat{\theta}, \tag{15}$$

with $\hat{\theta} = \begin{bmatrix} \hat{\theta}_1 & \hat{\theta}_2 & \hat{\theta}_3 & \hat{\theta}_4 & \hat{\theta}_5 & \hat{\theta}_6 & \hat{\theta}_7 & \hat{\theta}_8 \end{bmatrix}^T$,

$$\delta_1 = \dot{u}_{0_{ref}}^k + k_u\tilde{u}, \qquad k_u > 0, \tag{16}$$

and

$$\delta_2 = \dot{\omega}^k_{0_{ref}} + k_\omega \tilde{\omega}, \qquad k_\omega > 0, \tag{17}$$

where $\tilde{u} = u^k_{0_{ref}} - u_0$ and $\tilde{\omega} = \omega^k_{0_{ref}} - \omega_0$.

The reference velocities $u^k_{0_{ref}}$ and $\omega^k_{0_{ref}}$ and the feedback data are handled by the dynamic controller according to equations (16) and (17), to generate the control signals δ_1 and δ_2 to be applied to the robot, configuring the inner-outer loops control architecture [19], [23], also known as a cascade one.

Continuing with the discussion on dynamic compensation, if the estimated parameters of the controller in (15) ($\hat{\theta}_i, i = 1, \cdots, 8$) match those of the dynamic model (refer to (13)), then the compensation represents a perfect inversion of the model. However, in scenarios where uncertainties exist in the actual parameters of the MARV or variations occur during navigation, such as adding or dropping out a load, the fixed parameters of the dynamic compensation become insufficient to mitigate navigation errors. In such cases, it becomes advantageous to implement a parameter adaptation law to adjust the dynamic controller and compensate for parameter variations, as elaborated further.

A. PARAMETERS ADAPTATION LAW

The adaptive control scheme integrates a regulation mechanism to adjust the parameters $\hat{\theta}$ of the dynamic controller described in (15). This adjustment relies on the dynamic model specified in (14).

First of all, the control law in (15) can be reformulated as

$$\mathbf{v_{ref}} = \hat{\mathbf{D}}^\dagger \delta + \hat{\eta}^\dagger, \tag{18}$$

where $\delta = \begin{bmatrix}\delta_1 & \delta_2\end{bmatrix}^T$,

$$\hat{\mathbf{D}}^\dagger = diag(\hat{\theta}1 + \hat{\theta}7|cos\gamma_1|, \hat{\theta}2 + \hat{\theta}8|sin\gamma_1|),$$

and

$$\hat{\eta}^\dagger = \mathbf{B}^\dagger \begin{bmatrix}\hat{\theta}_1 & \hat{\theta}_2 & \hat{\theta}_3 & \hat{\theta}_4 & \hat{\theta}_5 & \hat{\theta}_6 & \hat{\theta}_7 & \hat{\theta}_8\end{bmatrix}^T.$$

If $\hat{\theta}_i = \theta_i$, $i = 1, \cdots, 8$, then $\hat{\mathbf{D}}^\dagger = \mathbf{D}^\dagger$, $\hat{\eta}^\dagger = \eta^\dagger$, and the dynamic controller perfectly inverses the model. However, typically, the $\hat{\theta}$ estimates of the parameters θ include uncertainties, which can fluctuate with changes in trailer payload, for example. Consequently, the dynamic controller generally contains inherent errors, which can be mitigated by updating laws for the estimated parameters.

Manipulating (18), one can write

$$\mathbf{v}_{ref} = \mathbf{G}(\delta_1, \delta_2, u_0, w_0)\hat{\theta}, \tag{19}$$

where

$$\mathbf{G} = \begin{bmatrix}\delta_1 & 0 & -\omega_0^2 & u_0 & 0 & 0 & \phi_1 & 0 \\ 0 & \delta_2 & 0 & 0 & \omega_0 u_0 & \omega_0 & 0 & \phi_2\end{bmatrix}, \tag{20}$$

with $\phi_1 = \delta_1|cos\gamma_1|$ and $\phi_2 = \delta_2|sin\gamma_1|$. Introducing uncertainties in the parameters, (19) becomes

$$\mathbf{v}_{ref} = \mathbf{G}\hat{\theta} = \mathbf{G}\theta + \mathbf{G}\tilde{\theta} = \mathbf{D}^\dagger\delta + \eta^\dagger + \mathbf{G}\tilde{\theta}, \tag{21}$$

where $\tilde{\theta} = \hat{\theta} - \theta$ denotes an unknown deviation between the estimated and real values. The adaptive controller aims to reduce such discrepancies over time.

For parameter updating, the sigma-modification law [24, p 253] is considered, which adds to the typical gradient law a term aimed at preventing parameter drift. The parameter updating law is then

$$\dot{\hat{\theta}} = \lambda^{-1}\mathbf{G}^T\tilde{\mathbf{v}} - \lambda^{-1}\mathrm{o}\hat{\theta}, \tag{22}$$

where $\lambda, \mathrm{o} \in \mathbb{R}^{8\times8}$ are positive definite diagonal matrices, $\tilde{\mathbf{v}} = \mathbf{v}^k_{ref} - \mathbf{v}$, $\mathbf{v}^k_{ref} = \begin{bmatrix}u^k_{0ref} & \omega^k_{0ref}\end{bmatrix}^T$, and $\mathbf{v} = \begin{bmatrix}u_o & \omega_0\end{bmatrix}^T$. This updating process begins with the initial estimate of $\hat{\theta}$ in Section II-E, incorporating additional terms $\theta_7 = \theta_8 = 0.1$, which are empirically set due to the limited data available from open-loop MARV navigation in reverse motions. Initially, using only $\hat{\theta}$ introduces errors in the system response, which gradually decrease with the parameter updating law.

Therefore, the diagram of the whole controller proposed here is shown in Figure 3, which is reproduced from [11]. The only difference is that here the dynamic compensator is based on $\hat{\theta} = \begin{bmatrix}\hat{\theta}_1, & \cdots, & \hat{\theta}_8\end{bmatrix}^T$. However, for the sake of comparison, such a controller has also been run considering $\hat{\theta} = \begin{bmatrix}\hat{\theta}_1, & \cdots, & \hat{\theta}_6\end{bmatrix}^T$.

B. STABILITY ANALYSIS

The stability of the control system when adopting the proposed dynamic compensation is now analyzed. To close the loop means to equate (21) and (14). By doing that, one gets

$$\mathbf{D}^\dagger\dot{\mathbf{v}} + \eta^\dagger = \mathbf{D}^\dagger\delta + \eta^\dagger + \mathbf{G}\tilde{\theta}, \tag{23}$$

and, after rearranging the terms,

$$\mathbf{D}^\dagger(\delta - \dot{\mathbf{v}}) = -\mathbf{G}\tilde{\theta}. \tag{24}$$

Considering $\delta = \dot{\mathbf{v}}_{ref} + \mathbf{K}\tilde{\mathbf{v}}$ (see (16) and (17)), where $\mathbf{K}$ is a diagonal positive definite gain matrix, and $\tilde{\mathbf{v}} = \mathbf{v}_{ref} - \mathbf{v}$, one gets $\delta - \dot{\mathbf{v}} = \dot{\tilde{\mathbf{v}}} + \mathbf{K}\tilde{\mathbf{v}}$, and, therefore,

$$\mathbf{D}^\dagger(\dot{\tilde{\mathbf{v}}} + \mathbf{K}\tilde{\mathbf{v}}) = -\mathbf{G}\tilde{\theta} \tag{25}$$

or

$$\dot{\tilde{\mathbf{v}}} = -\mathbf{D}^{\dagger^{-1}}\mathbf{G}\tilde{\theta} - \mathbf{K}\tilde{\mathbf{v}}. \tag{26}$$

Taking into account the theory of Lyapunov, let the Lyapunov candidate function be

$$V = \frac{1}{2}\tilde{\mathbf{v}}^T\mathbf{D}^\dagger\tilde{\mathbf{v}} + \frac{1}{2}\tilde{\theta}^T\lambda\tilde{\theta}, \tag{27}$$

where $\tilde{\theta} = \hat{\theta} - \theta$. Notice that such a Lyapunov candidate function is feasible because $\mathbf{D}^\dagger > 0$, according to the discussion about the new dynamic model considering 8 parameters. Notice that this is true whenever the MARV is not in a jackknife condition, which means in normal operation. Therefore, $\gamma_1 < 90°$, and the parameters $\theta_7|cos\gamma_1|$ and $\theta_8|sin\gamma_1|$ are always positive. This guarantees that $\mathbf{D}^\dagger >$

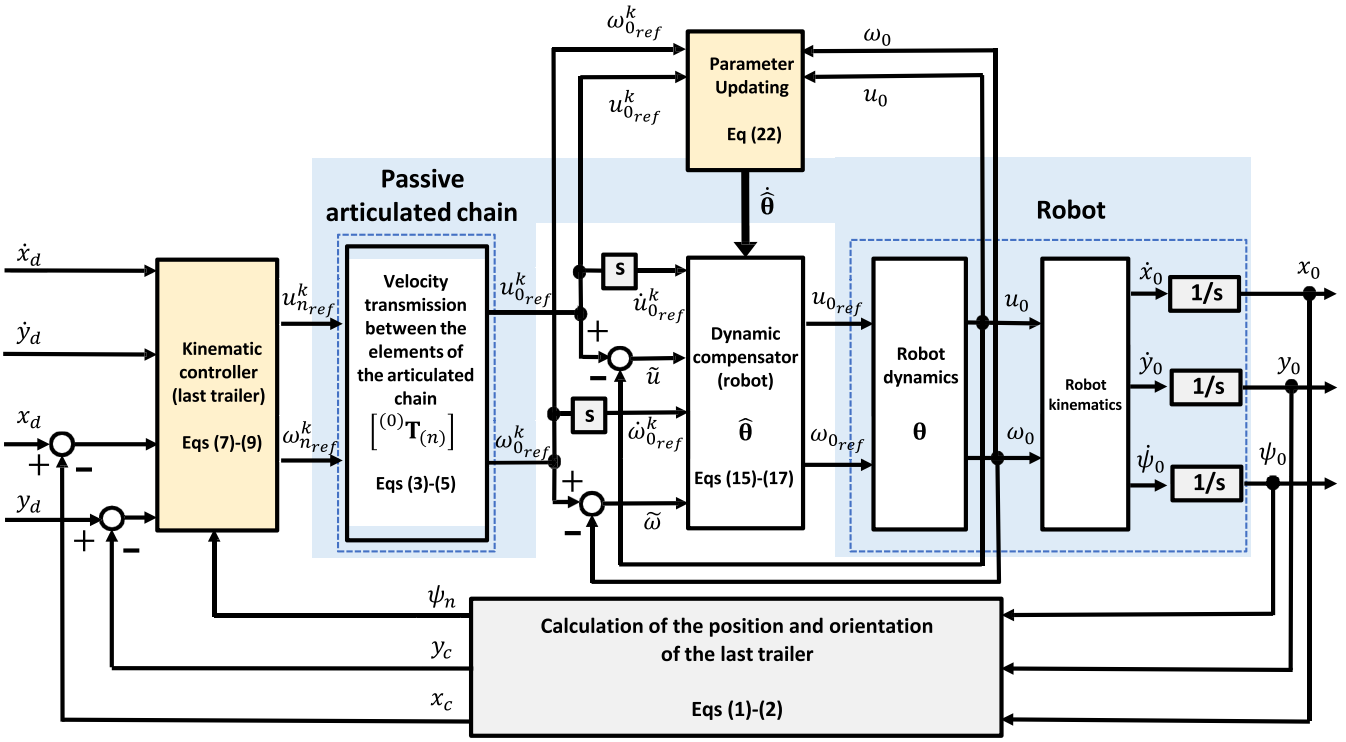


FIGURE 3. Block diagram of the whole controller (reproduced from [11] and adapted).

0 as well as λ, arbitrarily chosen to be a positive definite matrix. As for the time derivative of such a function, it is

$$\dot{V} = \tilde{\mathbf{v}}^T \mathbf{D}^\dagger \dot{\tilde{\mathbf{v}}} + \frac{1}{2}\tilde{\mathbf{v}}^T \dot{\mathbf{D}}^\dagger \tilde{\mathbf{v}} + \tilde{\theta}^T \lambda \dot{\tilde{\theta}}. \tag{28}$$

Introducing (26) in (28) it comes

$$\dot{V} = -\tilde{\mathbf{v}}^T \mathbf{D}^\dagger \mathbf{K} \tilde{\mathbf{v}} + \frac{1}{2}\tilde{\mathbf{v}}^T \dot{\mathbf{D}}^\dagger \tilde{\mathbf{v}} - \tilde{\mathbf{v}}^T \boldsymbol{G} \tilde{\theta} + \tilde{\theta}^T \lambda \dot{\tilde{\theta}}. \tag{29}$$

Now, assuming θ constant and using the sigma modification adaptation law $\dot{\tilde{\theta}} = \dot{\hat{\theta}} = \lambda^{-1}\mathbf{G}^T\tilde{\mathbf{v}} - \lambda^{-1}\mathrm{o}\hat{\theta}$, which can be rewritten as

$$\dot{\tilde{\theta}} = \dot{\hat{\theta}} = \lambda^{-1}\mathbf{G}^T\tilde{\mathbf{v}} - \lambda^{-1}\mathrm{o}\tilde{\theta} - \lambda^{-1}\mathrm{o}\theta, \tag{30}$$

and substituting (30) in (29) one gets

$$\dot{V} = -\tilde{\mathbf{v}}^T \mathbf{D}^\dagger \mathbf{K} \tilde{\mathbf{v}} + \frac{1}{2}\tilde{\mathbf{v}}^T \dot{\mathbf{D}}^\dagger \tilde{\mathbf{v}} - \tilde{\theta}^T \mathrm{o}\tilde{\theta} - \tilde{\theta}^T \mathrm{o}\theta. \tag{31}$$

Now, choosing $\mathbf{K}$ such that $||\mathbf{K}|| > \frac{1}{2}||\mathbf{D}^{\dagger^{-1}}||||\dot{\mathbf{D}}^\dagger|| + \zeta$, with $\zeta > \mathbf{0}$, one concludes that

$$\dot{V} \leq -\tilde{\mathbf{v}}^T \zeta \tilde{\mathbf{v}} - \tilde{\theta}^T \mathrm{o}\tilde{\theta} - \tilde{\theta}^T \mathrm{o}\theta. \tag{32}$$

Considering the constants $\mu_\zeta = \sigma(\zeta)$ and $\mu_\mathrm{o} = \sigma(\mathrm{o})$, where $\sigma(\boldsymbol{A}) = \sqrt{\lambda_{min}(\boldsymbol{A}^T\boldsymbol{A})}$ is the minimum singular value of $\boldsymbol{A}$, whereas $\lambda_{min}(.)$ is the smallest eigenvalue of a matrix, it results that

$$\dot{V} \leq -\mu_\zeta \left\|\tilde{\mathbf{v}}\right\|^2 - \mu_\mathrm{o}\|\tilde{\theta}\|^2 + \mu_\mathrm{o}\|\tilde{\theta}\|\,\|\theta\|\,. \tag{33}$$

Considering the squared difference

$$\left(\frac{1}{\varphi}\|\tilde{\theta}\| - \varphi\,\|\theta\|\right)^2 = \frac{1}{\varphi^2}\|\tilde{\theta}\|^2 - 2\|\tilde{\theta}\|\,\|\theta\| + \varphi^2\,\|\theta\|^2\,, \tag{34}$$

where $\varphi \in \mathbb{R}^+$, it can be written that

$$\|\tilde{\theta}\|\,\|\theta\| = \frac{1}{2\varphi^2}\|\tilde{\theta}\|^2 + \frac{\varphi^2}{2}\|\theta\|^2 - \frac{1}{2}\left(\frac{1}{\varphi}\|\tilde{\theta}\| - \varphi\,\|\theta\|\right)^2. \tag{35}$$

Disregarding the negative term, the inequality

$$\|\tilde{\theta}\|\,\|\theta\| \leq \frac{1}{2\varphi^2}\|\tilde{\theta}\|^2 + \frac{\varphi^2}{2}\|\theta\|^2 \tag{36}$$

is obtained, and after replacing (36) in (33) one gets

$$\dot{V} \leq -\mu_\zeta \left\|\tilde{\mathbf{v}}\right\|^2 - \mu_\mathrm{o}\|\tilde{\theta}\|^2 + \mu_\mathrm{o}\left(\frac{1}{2\varphi^2}\|\tilde{\theta}\|^2 + \frac{\varphi^2}{2}\|\theta\|^2\right), \tag{37}$$

or,

$$\dot{V} \leq -\mu_\zeta \left\|\tilde{\mathbf{v}}\right\|^2 - \mu_\mathrm{o}\left(1 - \frac{1}{2\varphi^2}\right)\|\tilde{\theta}\|^2 + \mu_\mathrm{o}\frac{\varphi^2}{2}\|\theta\|^2\,. \tag{38}$$

In the sequence, the parameters $\alpha_1 = \mu_\zeta > 0$ and $\alpha_2 = \mu_o\left(1 - \frac{1}{2\varphi^2}\right) > 0$ are defined, with φ conveniently selected. Then, (38) can be rewritten as

$$\dot{V} \leq -\alpha_1 \left\|\tilde{\mathbf{v}}\right\|^2 - \alpha_2 \|\tilde{\theta}\|^2 + \rho, \tag{39}$$

where $\rho = \mu_o \frac{\varphi^2}{2} \|\theta\|^2$.

Now, equation (27) can be stated as

$$V \leq \beta_1 \left\|\tilde{\mathbf{v}}\right\|^2 + \beta_2 \|\tilde{\theta}\|^2, \tag{40}$$

where $\beta_1 = \frac{1}{2}\upsilon_{\mathbf{D}^\dagger}$, $\beta_2 = \upsilon_\lambda$, with $\upsilon_\lambda = \kappa_{max}(\lambda)$, $\upsilon_{\mathbf{D}^\dagger} = \kappa_{max}(\mathbf{D}^\dagger)$, with $\kappa_{max}(\mathbf{A}) = \sqrt{\lambda_{max}(\mathbf{A}^T\mathbf{A})}$ denoting the maximum singular value of the matrix $\mathbf{A}$. Then,

$$\dot{V} \leq -\Lambda V + \rho \tag{41}$$

with $\Lambda = min\left\{\frac{\alpha_1}{\beta_1}, \frac{\alpha_2}{\beta_2}\right\}$.

Given that ρ is bounded, (41) allows concluding that both $\tilde{\mathbf{v}}(t)$ and $\tilde{\theta}(t)$ are ultimately bounded. Consequently, the sigma modification enhances the robustness of the adaptation law compared to the conventional derivative law, albeit at the cost of enlarging the error threshold. Since ρ depends on the smallest singular value of the gain matrix o in the sigma-modification term and can take arbitrary values, it is feasible to minimize the error threshold. In theory, as o approaches zero, it can be demonstrated that $\tilde{\mathbf{v}}$ tends to zero as t approaches infinity.

Remark 1: Let us consider the dynamic model (14) and include a term ξ representing bounded unmodeled dynamics and disturbances. Then, (26) becomes,

$$\dot{\tilde{\mathbf{v}}} = -\mathbf{D}^{\dagger^{-1}}\mathbf{G}\tilde{\theta} - \mathbf{K}\tilde{\mathbf{v}} + \mathbf{D}^{\dagger^{-1}}\xi.$$

Through an analysis similar to the one previously done, we can get a new version of (39), in the form

$$\dot{V} \leq -\alpha_1 \left\|\tilde{\mathbf{v}}\right\|^2 - \alpha_2 \|\tilde{\theta}\|^2 + \rho + ||\tilde{\mathbf{v}}||||\xi||,$$

from where we immediately conclude that the control error $\tilde{\mathbf{v}}$ is ultimately bounded under the condition

$$\alpha_1 ||\tilde{\mathbf{v}}||^2 < ||\tilde{\mathbf{v}}||||\xi|| + \rho.$$

As can be seen, considering bounded unmodelled dynamics and disturbances, an exponential decrease in the errors cannot be proved, as in the previous analysis; however, the ultimate boundedness shows a robustness property of the controller to bounded disturbances and unmodelled dynamics.

IV. RESULTS

The results presented in this section were acquired in indoor experiments by controlling a tractor-trailer system to track a specified trajectory, a Bernoulli lemniscate characterized by $x_d(t) = 2\sin(2\pi t/60)\ m$, and $y_d(t) = 1.5\sin(4\pi t/60)\ m$. For such a trajectory the maximum velocity in the x direction is $\dot{v}_{xd_M} = 0.2091\ m/s$, while for the y direction it is $\dot{v}_{yd_M} = 0.3141\ m/s$, which corresponds to the maximum values of the time derivative of the desired trajectory (in trajectory-tracking tasks the velocity of the robot is the velocity of the trajectory). The MARV should complete five laps along the trajectory in each experiment trial. Two sets of trials were run: the first considered the dynamics of the tractor robot modeled using six parameters, as in [11], and the second considered the new model discussed here, with eight parameters. Each set of trials involved load changing from zero to 35 Kg in steps of 5 Kg, so that the whole experiment consisted of $2 \times 8 \times 5$ laps of the MARV. Moreover, each set of trials was repeated three times. The experiment was standardized to obtain comparable results. This way, the only change is the number of parameters used to model the dynamics of the tractor robot, increasing from six to eight. The movements always started with $\hat{\theta} = 0.5\theta$ to start the adaptation process with wrong parameters. In addition, since the maneuvers were performed with load changes throughout the movement, it was decided to begin the adaptation process at $t = 30$ s to exclude the data corresponding to the time it takes for the MARV to reach the trajectory.

The physical parameters of interest for the MARV are $L_{0_0} = 0.30$ m, $L_1 = 0.455$ m, and $b = 0.20$ m, featuring an off-axle hitch type. In particular, the dimensions of the trailer are 40 *cm* in length (65 *cm* if including the off-axle hitching stick), 28 *cm* in width (46 *cm* if including the tires), 15.5 *cm* in height (29 *cm* of total height, including the wheels), and 21 *cm* in wheel diameter, including the tires, with the total mass of approximately 4 Kg, when not loaded. In terms of sensing, each trailer contains a potentiometer to measure the angle between two adjacent elements of the chain, $\gamma_i,\ i = 1, \cdots, n$ (see Figure 1). However, for the experiments here reported, such angles were estimated using the motion capture system. The gains involved are $k_u = k_\omega = 4$ and $K_1 = K_2 = 0.8$, $\lambda^{-1} = diag[2.50\ 0.42\ 50\ 50\ 50\ 50\ 1\ 1] \times 10^{-5}$ and $o = 0.1 \times \lambda^{-1}$, with the sampling time of 100 ms. Finally, all trial runs began with the vehicle in the same initial position and orientation.

To collect the positions of the PoI along the experiment, the test arena depicted in Figure 4 was used. Such an arena features an installation of the motion capture system *OptiTrack*, comprising twelve full HD cameras. These cameras visually measure the current position and orientation of the tractor-trailer system with high accuracy, allowing for the determination of the position error relative to the desired positions specified in the lemniscate. In addition to Figure 4, Figure 5 shows four snapshots taken during one of the trial runs, in which the trailer is loaded, as part of the experiment.

As mentioned above, three experiments were conducted with the model containing six parameters, and the same procedure was repeated for the model with eight parameters for each load. Eight different loads were used, namely, 0 kg, 5 kg, 10 kg, 15 kg, 20 kg, 25 kg, 30 kg and 35 kg. Thus, a total of forty-eight maneuvers were performed. The IAE (Integral of the Absolute Error) index was adopted to compare performances, and the corresponding values were calculated

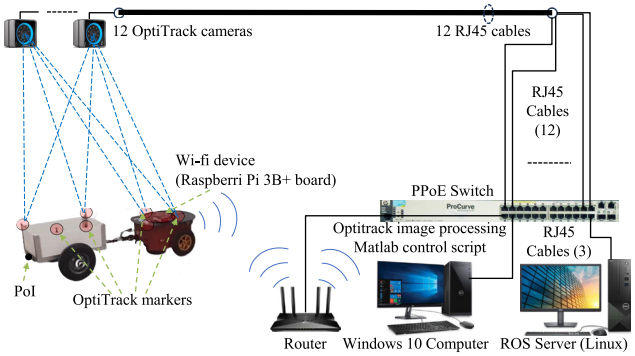


FIGURE 4. The test arena where the experiment was run.

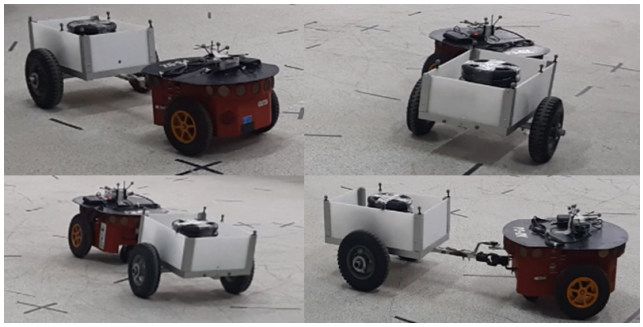


FIGURE 5. Four snapshots of the robot-trailer composition transporting a load of 20 Kg during one of the experiment trails.

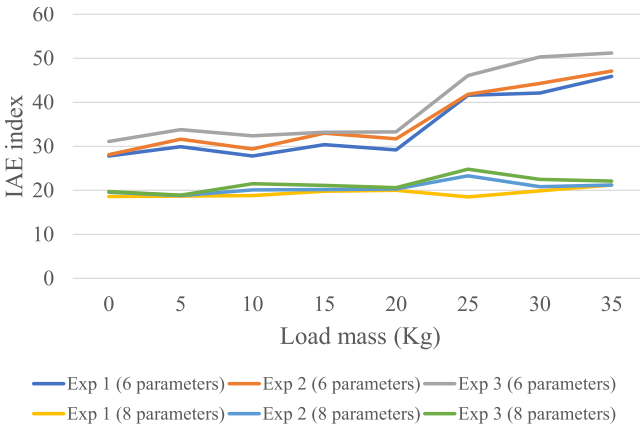


FIGURE 6. Error index IAE for a MARV pushing a single trailer with a load.

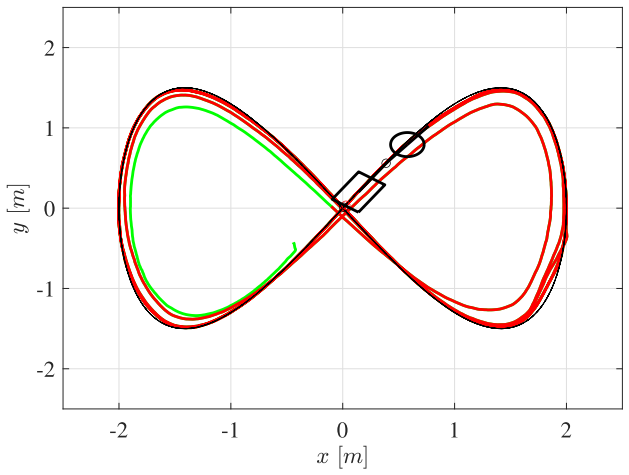
between the time instants $t = 150\,\text{s}$ and $t = 300\,\text{s}$, thus comprising a stage of the movement in which the parameters had already converged. Figure 6 shows a graphic of the IAE indexes obtained for the three experiments run considering the controller designed according to the model of six parameters and for the three experiments run considering the controller designed according to the new model here considered for the tractor element of the MARV.

As shown in the figure, the average reduction in the IAE index when using the proposed model for the tractor robot is approximately 40%, considering all trials. This indicates that the 8-parameter model captures some dynamic effects that are effectively present in the system but are not addressed when adopting the simplified 6-parameter model. As expected, the interaction trailer-tractor is not represented when considering the model with only six parameters. However, it has already been proven that even by adopting this more simplified model, the controller finds parameter values that produce low navigation errors [11], at least for low-mass loads. Nonetheless, the results of the 8-parameter model, which considers some interaction between the trailer and the tractor, show that this is a much better option. Moreover, as shown in Figure 6, the 8-parameter model exhibits significantly lower growth in the IAE index compared to the results obtained when the model with six parameters is used.

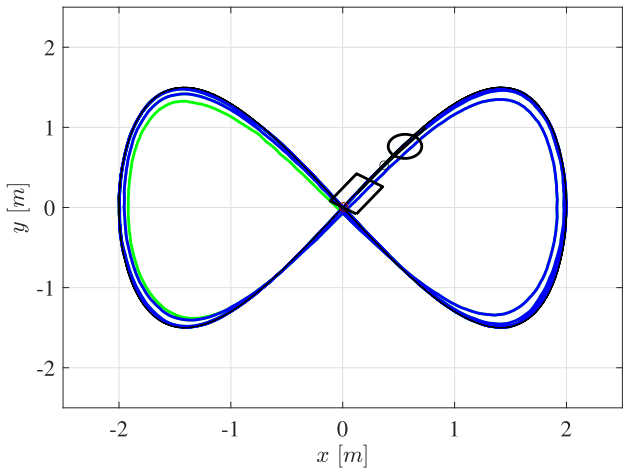
To reinforce these results, Figure 7 shows the desired (black line) and the effectively traveled routes for the MARV along one of the trials when the payload was 30 kg for the controllers based on the six-parameter (red line) and the eight-parameter (blue line) models. For such a figure, one can notice the difference in the effectively traveled routes, with greater errors associated with the six-parameter model. However, the green segment, in both cases, should not be considered because it corresponds to the time before the adaptation begins to work. Moreover, Figure 8 shows the distance of the robot to the trajectory being tracked during navigation for the six-parameter (red line) and eight-parameter (blue line) models, clearly indicating that the error is larger for the six-parameter model. In this case, the time interval before adaptation (corresponding to the green segment of both cases depicted in Figure 7), the first 30 s should be disregarded.

To conclude the analysis of the controller's performance, designed considering the influence of the trailer on the tractor for the MARV, an animation is available at https://youtu.be/ESVCMuzALYU. The video consists of two parts: the first part considers the controller designed using the six-parameter MARV model, and the second part considers the controller designed using the eight-parameter MARV model proposed in this work. The animation was built using the data corresponding to the desired trajectory (black line, present in the two parts of the video), the controller based on the six-parameter model (red line, present in the first part of the video) and the controller based on the eight-parameter model (blue line, present in the second part of the video), when considering the same experiment of Figures 7 and 8. Once more, the green part of the route traveled by the MARV, in both parts of the video, corresponds to the time interval before the adaptation starts.

Finally, it is important to justify why the experiment was not repeated for an MARV with two trailers. First, the test arena has an area of about $30\,\text{m}^2$, insufficient to perform the same maneuvers. A second point is that the tractor robot adopted can not push much more than the 35 Kg used for the first trailer. This way, the experiment only considered the case of one trailer. However, we believe that this experiment



(a) 6-parameter model



(b) 8-parameter model

FIGURE 7. Routes traveled by the MARV when using the six-parameter (red line, in part a) and the eight-parameter (blue line, in part b) models. The black line, present in both parts of the figure, is the desired route.

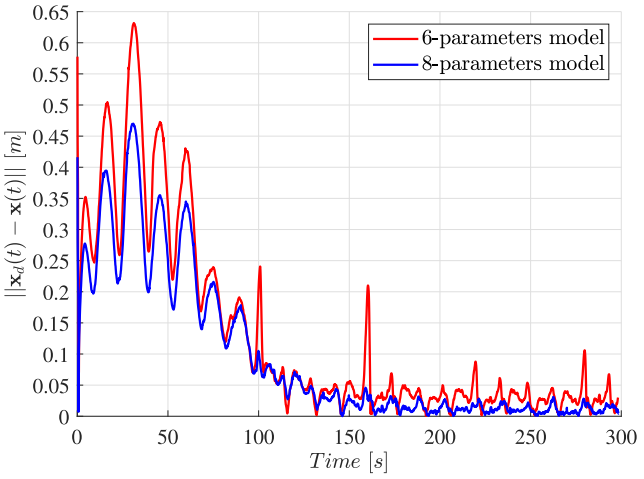


FIGURE 8. Distance MARV-trajectory when using the six-parameter and the eight-parameter models.

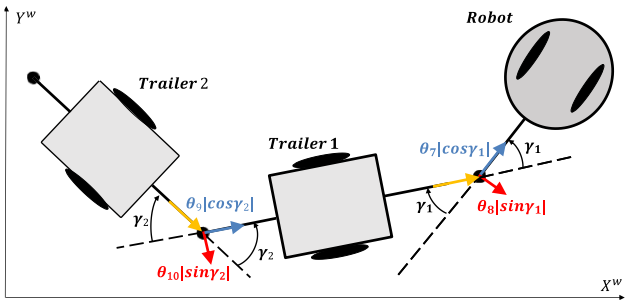


FIGURE 9. Accounting for the effect of two trailers on the tractor robot.

is enough to support our proposal of using more parameters to represent the dynamics of the tractor robot when pushing trailers.

V. THE MARV WITH *N* TRAILERS

Considering that all the influence of the trailers is concentrated in the first one, it is equivalent to considering just a single trailer, akin to a tractor-trailer configuration. Now, we are considering additional trailers to generalize the eight-parameter dynamic model for the tractor robot. First, as Figure 9 illustrates, we consider two trailers as an intermediate step to generalize to n trailers.

For such a case (14), namely,

$$\mathbf{v}_{ref} = \mathbf{D}^{\dagger}\dot{\mathbf{v}} + \eta^{\dagger}, \tag{42}$$

is still valid, now with

$$\mathbf{D}^{\dagger} = \begin{bmatrix} \chi_1 & 0 \\ 0 & \chi_2 \end{bmatrix},$$

where $\chi_1 = \hat{\theta}_1 + \hat{\theta}_7|cos\gamma_1| + \hat{\theta}_9|cos\gamma_2 cos\gamma_1|$ and $\chi_2 = \hat{\theta}_2 + \hat{\theta}_8|sin\gamma_1| + \hat{\theta}_{10}|cos\gamma_2 sin\gamma_1|$, and $\eta^{\dagger} = \mathbf{B}^{\dagger}\hat{\theta}$, where

$$\mathbf{B}^{\dagger} = \begin{bmatrix} 0 & 0 & -\omega_0^2 & u_0 & 0 & 0 & 0 & 0 & 0 & 0 \\ 0 & 0 & 0 & 0 & \omega_0 u_0 & \omega_0 & 0 & 0 & 0 & 0 \end{bmatrix}$$

and $\hat{\theta} = \begin{bmatrix} \hat{\theta}_1 & \hat{\theta}_2 & \hat{\theta}_3 & \hat{\theta}_4 & \hat{\theta}_5 & \hat{\theta}_6 & \hat{\theta}_7 & \hat{\theta}_8 & \hat{\theta}_9 & \hat{\theta}_{10} \end{bmatrix}^T$. Similarly to $\hat{\theta}_7$ and $\hat{\theta}_8$ in (14), $\hat{\theta}_9$ and $\hat{\theta}_{10}$ are also constants to be identified.

As one can see from the above dynamic model, the controller designed for the case of (14) is also valid for this case, as well as the stability proof, with the only difference being the order of the matrices involved.

Expanding the analysis associated to (42) to the case of n trailers, it is intuitive that such an equation remains valid, as well as the controller designed and the stability proof, now with

$$\chi_1 = \hat{\theta}_1 + \hat{\theta}_7|c_{\gamma_1}| + \hat{\theta}_9|c_{\gamma_2}c_{\gamma_1}| + \hat{\theta}_{11}|c_{\gamma 3}c_{\gamma_2}c_{\gamma_1}| + \cdots$$

and

$$\chi_2 = \hat{\theta}_2 + \hat{\theta}_8|s_{\gamma_1}| + \hat{\theta}_{10}|c_{\gamma_2}s_{\gamma_1}| + \hat{\theta}_{12}|c_{\gamma_3}c_{\gamma_2}s_{\gamma_1}| + \cdots,$$

with c_{γ_i} standing for $cos\gamma_i$ and s_{γ_i} standing for $sin\gamma_i$. As for the vector $\hat{\theta}$, it becomes

$$\hat{\theta} = \begin{bmatrix} \hat{\theta}_1 & \cdots & \hat{\theta}_6 & \hat{\theta}_7 & \hat{\theta}_8 & \hat{\theta}_9 & \hat{\theta}_{10} & \hat{\theta}_{11} & \hat{\theta}_{12} & \cdots \end{bmatrix}^T,$$

whereas the matrix $\mathbf{B}^{\dagger}$ receives additional columns of zeros, two for each new pair of parameters added, which means a pair of parameters for each new trailer. Therefore, the total number of parameters is six plus two for each trailer, which is the same number of columns of $\mathbf{B}^{\dagger}$.

VI. CONCLUSION

This work demonstrates that coupling a trailer to a differential robot, when adopted as the tractor element of a MARV, results in changes to its model. This was already expected, but modeling this new system is not a trivial task, and this work comes precisely to provide a simple and easy-to-implement alternative to this problem. Effectively, it was demonstrated that by incorporating two new parameters previously unknown into the dynamic model associated with the MARV tractor element, and utilizing adaptive dynamic control, it is possible to enhance MARV navigation during backward movements. This work demonstrates that for a single trailer, the most commonly used MARV configuration, increasing the number of parameters in the dynamic model of the tractor element is beneficial to account for the trailer's impact. The reason is that this results in much smaller navigation errors, even with an increased set of parameters to be adjusted by the parameter updating law associated with the adaptive controller. Moreover, the reported results show that when adopting the model with eight parameters, the error indices do not increase as the load transported by the MARV increases, which validates the usefulness of the trailer interaction model proposed in this study. The experiments have been carried out with a velocity considered normal. Executions with higher speeds would certainly increase the control errors, but also emphasize the advantages of the new parameterization proposal while incorporating the dynamic effects of the trailers.

This work also investigates how to consider the dynamic behavior of the tractor element of an MARV with multiple trailers. Specifically, it analyzes the case of two trailers, incorporating two additional parameters to model the dynamics of the tractor robot. The analysis concludes by proposing a generalization for a MARV with n trailers in the articulated chain. The paper demonstrates that the same controller can be adopted by simply enlarging the matrices involved. Therefore, the theoretical analysis made for one trailer remains valid, and the results obtained for one trailer can be generalized to n trailers.

As future research, it would be interesting to consider other kinematic structures both for the tractor and the trailers. For instance, consider a car-like robot as the tractor element, which is a more realistic case when considering real-world applications. Also, experiments in real-world environments, such as rough terrain, will be of interest.

REFERENCES

[1] M. A. Post, A. Bianco, and X. T. Yan, "Autonomous navigation with ROS for a mobile robot in agricultural fields," in *Proc. 14th Int. Conf. Informat. Control, Autom. Robot.*, 2017, pp. 79–87.

[2] J. David and P. V. Manivannan, "Control of truck-trailer mobile robots: A survey," *Intell. Service Robot.*, vol. 7, no. 4, pp. 245–258, Oct. 2014.

[3] A. W. Divelbiss and J. T. Wen, "Trajectory tracking control of a car-trailer system," *IEEE Trans. Control Syst. Technol.*, vol. 5, no. 3, pp. 269–278, May 1997.

[4] D. N. Bertolani, V. P. Bacheti, and M. Sarcinelli-Filho, "Controlling a unicycle mobile platform pushing 1 and 2 passive trailers," *J. Intell. Robotic Syst.*, vol. 103, no. 3, p. 43, Nov. 2021.

[5] K. Shojaei, "Neural network formation control of a team of tractor-trailer systems," *Robotica*, vol. 36, no. 1, pp. 39–56, Jan. 2018.

[6] Z. Jin, Z. Liang, P. Guo, and M. Zheng, "Adaptive backstepping tracking control of a car with n trailers based on RBF neural network," *Asian J. Control*, vol. 23, no. 2, pp. 824–834, Mar. 2021.

[7] A. Moran, "Autonomous path following of truck-trailer vehicles using linear-fuzzy control," in *Proc. 3rd Int. Conf. Control, Autom. Robot. (ICCAR)*, Apr. 2017, pp. 651–657.

[8] J. Cheng, B. Wang, Y. Zhang, and Z. Wang, "Backward orientation tracking control of mobile robot with n trailers," *Int. J. Control, Autom. Syst.*, vol. 15, no. 2, pp. 867–874, Apr. 2017.

[9] M. M. Michalek, "Cascade-like modular tracking controller for non-standard N-trailers," *IEEE Trans. Control Syst. Technol.*, vol. 25, no. 2, pp. 619–627, Mar. 2017.

[10] S. P. Kruglov and S. V. Kovyrshin, "Adaptive trailer backup control," in *Proc. Int. Multi-Conf. Ind. Eng. Modern Technol. (FarEastCon)*, Oct. 2018, pp. 1–6.

[11] D. N. Bertolani, V. P. Bacheti, A. S. Brandão, R. Carelli, and M. Sarcinelli-Filho, "Controlling a multi-articulated robot in backward movement using an adaptive controller," *Mechatronics*, vol. 92, Jun. 2023, Art. no. 102967.

[12] T. Nayl, G. Nikolakopoulos, T. Gustafsson, D. Kominiak, and R. Nyberg, "Design and experimental evaluation of a novel sliding mode controller for an articulated vehicle," *Robot. Auto. Syst.*, vol. 103, pp. 213–221, May 2018.

[13] M. Yue, X. Hou, R. Gao, and J. Chen, "Trajectory tracking control for tractor-trailer vehicles: A coordinated control approach," *Nonlinear Dyn.*, vol. 91, no. 2, pp. 1061–1074, Jan. 2018.

[14] O. Ljungqvist, D. Axehill, H. Pettersson, and J. Löfberg, "Estimation-aware model predictive path-following control for a general 2-trailer with a car-like tractor," 2020, *arXiv:2002.10291*.

[15] M. Yue, X. Wu, L. Guo, and J. Gao, "Quintic polynomial-based obstacle avoidance trajectory planning and tracking control framework for tractor-trailer system," *Int. J. Control, Autom. Syst.*, vol. 17, no. 10, pp. 2634–2646, Oct. 2019.

[16] M. Sarcinelli-Filho and R. Carelli, "Kinematic models," in *Control of Ground and Aerial Robots*. Cham, Switzerland: Springer, 2023, ch. 2, pp. 12–14.

[17] J. Morales, A. Mandow, J. L. Martinez, J. L. Martínez, and A. J. García-Cerezo, "Driver assistance system for backward maneuvers in passive multi-trailer vehicles," in *Proc. IEEE/RSJ Int. Conf. Intell. Robots Syst.*, Oct. 2012, pp. 4853–4858.

[18] J. Morales, J. L. Martinez, A. Mandow, and A. J. Garcia-Cerezo, "Steering the last trailer as a virtual tractor for reversing vehicles with passive on- and off-axle hitches," *IEEE Trans. Ind. Electron.*, vol. 60, no. 12, pp. 5729–5736, Dec. 2013.

[19] M. Sarcinelli-Filho and R. Carelli, "Motion control," in *Control of Ground and Aerial Robots*. Cham, Switzerland: Springer, 2023, ch. 4, pp. 44–47.

[20] M. Sarcinelli-Filho and R. Carelli, "Dynamic models," in *Control of Ground and Aerial Robots*. Cham, Switzerland: Springer, 2023, ch. 3, pp. 23–29.

[21] F. N. Martins, W. C. Celeste, R. Carelli, M. Sarcinelli-Filho, and T. F. Bastos-Filho, "An adaptive dynamic controller for autonomous mobile robot trajectory tracking," *Control Eng. Pract.*, vol. 16, no. 11, pp. 1354–1363, Nov. 2008.

[22] F. N. Martins, M. Sarcinelli-Filho, and R. Carelli, "A velocity-based dynamic model and its properties for differential drive mobile robots," *J. Intell. Robotic Syst.*, vol. 85, no. 2, pp. 277–292, Feb. 2017.

[23] N. Cao and A. F. Lynch, "Inner–outer loop control for quadrotor UAVs with input and state constraints," *IEEE Trans. Control Syst. Technol.*, vol. 24, no. 5, pp. 1797–1804, May 2016.
[24] S. Sastry and M. Bodson, *Adaptive Control: Stability, Convergence, and Robustness*. Upper Saddle River, NJ, USA: Prentice-Hall, 1989.



DIEGO NUNES BERTOLANI received the B.S. degree in computer engineering and the M.Sc. and Ph.D. degrees in electrical engineering from the Federal University of Espírito Santo, Brazil, in 2011, 2013, and 2023, respectively. His research interests include controlling multi-articulated robotic vehicles (MARVs) and multi-robot systems composed of a MARV and an aerial robot.



RICARDO CARELLI (Senior Member, IEEE) received the degree in engineering from the National University of San Juan, Argentina, and the Ph.D. degree in electrical engineering from the National University of Mexico (UNAM). He is currently a Full Professor at the National University of San Juan and a Senior Researcher at the National Scientific and Technical Research Council of Argentina (CONICET). He has co-authored over 110 journal articles and more than 220 conference papers, as well as 18 book chapters. His research interests include robotics, adaptive control, and artificial intelligence applied to automatic control. He is a member of AADECA-IFAC.



MÁRIO SARCINELLI-FILHO received the B.S. degree in electrical engineering from the Federal University of Espírito Santo, Brazil, in 1979, and the M.Sc. and Ph.D. degrees in electrical engineering from the Federal University of Rio de Janeiro, Brazil, in 1983 and 1990, respectively. He is currently a Professor at the Department of Electrical Engineering, Federal University of Espírito Santo and a Researcher with Brazilian National Council for Scientific and Technological Development (CNPq). He has authored two books, co-authored over 80 journal articles, more than 400 conference papers, and 17 book chapters, besides having advised 23 Ph.D. and 29 M.Sc. students. His research interests include nonlinear control, mobile robot navigation, coordinated control of mobile robots, uncrewed aerial vehicles, multi-articulated robotic vehicles, and ground and aerial robot coordination. He is a member of the Executive Advisory Board of *Journal of Intelligent and Robotic Systems*, a Senior Member of Brazilian Society of Automatics, and an IFAC National Member Organization. He is an Associate Editor of *Journal of Control, Automation and Electrical Systems*.

Coordenação de Aperfeiçoamento de Pessoal de Nível Superior (CAPES) - ROR identifier: 00x0ma614